Supporting information:
Numerical investigation on the dynamic behavior of bubbles under forced flow in a microchannel

Dayong Li, Junbo Xing, Ziqun Zhang, Hongfei Wang*

School of Electromechanical and Automotive Engineering, Yantai University, Yantai, 264005 China;

Corresponding Author: dayongli@ytu.edu.cn

Analysis of the estimated force trends for surface bubble sliding and detaching: when the sum of shear lift force $\mathbf{F}_{sl}$, buoyancy force $\mathbf{F}_b$ and contact pressure force $\mathbf{F}_{cp}$ becomes substantially larger than the pinning force component $\mathbf{F}_{py}$ in the y-direction (i.e., $\sum \mathbf{F}_y > 0$), the surface bubble detaches from the wall. Meanwhile, if the fluid flow force $\mathbf{F}_{qs}$ exceeds the x-direction pinning force component $\mathbf{F}_{px}$, the bubble will slide along the x-axis.

Specifically, the drag force $\mathbf{F}_{qs}$ shows an increase which can be judged from the flow field in Figure 4 in the manuscript (Fig. S1a). As the three-phase contact line contracts, the bubble height increases. Since the fluid velocity increases parabolically from the wall to the channel center, this height increase subjects the bubble to higher fluid forces due to the increased flow velocity. Consequently, the term $R^2(u-v)|u-v|$ in formula 12 increases. Based on equation 13 in the manuscript, we can conclude that the shear lift force $\mathbf{F}_{sl}$ acting on the bubble also increases.

The variation of contact pressure $\mathbf{F}_{cp}$ during the sliding of surface bubbles and their transformation into bulk bubbles can be determined by formula 14 in the manuscript, which can be expressed as

$$\mathbf{F}_{cp} = \frac{\pi d_w^2}{4} \cdot \frac{2\gamma_{\mathrm{lg}}}{R} \tag{1}$$

Here d_w is the base diameter of a surface bubble on the channel wall, γ_{lg} is the surface tension of gas-liquid interface. For a spherical cap-shaped surface bubble, its volume can be calculated using the following formula

$$V = \frac{\pi h^2 (3R - h)}{3} \tag{2}$$

Where, R represents the curvature radius of the sphere, and h represents the height of the spherical cap. Assuming the bubble volume remains constant, R can be expressed as a function of h, i.e., $R = \frac{3V}{\pi h^2} + \frac{h}{3}$. Thus the ratio of ${d_w}^2$ to R can be expressed as

$$\frac{d_w^2}{R} = 8h - \frac{4h^2}{R} \tag{3}$$

Substitute $R = \frac{3V}{\pi h^2} + \frac{h}{3}$ into the formula 3, we obtain

$$\frac{{d_w}^2}{R} = 8h - \frac{12h^4}{h^3 + C} \tag{4}$$

Here, constant $C = \frac{9V}{\pi}$. To find the derivative of $f(h) = 8h - \frac{12h^4}{h^3 + C}$ at the point 0, i.e., $f'(h) = 8 - \frac{12h^3(h^3 + 4C)}{(h^3 + C)^2} = 0$, we get $h_0 = [(-4 + 3\sqrt{2})C]^{1/3}$. When h increases from its initial value to h_0, $\frac{{d_w}^2}{R}$ becomes monotonically increasing, while h increases from h_0 to $2R$; $\frac{{d_w}^2}{R}$ decreases monotonically until it reaches 0 at $h = 2R$, indicating that the contact pressure force $\mathbf{F}_{cp}$ increase first and then decrease during the process of surface bubble detachment.

The buoyancy force $\mathbf{F}_b$ acting on a surface gas bubble is estimated according to Archimedes principle and can be expressed as (equation 15 in the manuscript)

$$\mathbf{F}_b = V(\rho_l - \rho_g)g \tag{5}$$

During the contraction of three phase contact line of surface bubble, the bubble curvature radius R decrease, leading to an increase in the bubble inner pressure and thus a larger bubble volume V. Therefore, the buoyancy force $\mathbf{F}_b$ increases.

The pinning force $\mathbf{F}_p$ can be calculated based on the equation 16 in the manuscript, but this would demand highly precise measurements of dynamic bubble morphology parameters. These parameters encompass the surface area, volume, and the geometric characteristics of the three-phase contact line, these measurements are inherently intricate. Therefore, Here we evaluate the pinning force $\mathbf{F}_p$ qualitatively by analyze the change in length of bubble three-phase contact line. The three-phase contact line of surface bubbles shows obvious contraction during sliding and detaching, the length of bubble contact line decreases, leading to decrease in $\mathbf{F}_p$.

When the lower wall is rendered hydrophobic with a wetting angle of 135° (Fig. 8c in the manuscript, Fig. S1b), the surface gas bubble maintains its attachment to the wall, undergoing a reduction in height and sliding along the surface without detachment. It is noted that during the period from 0 ns to 400 ns, the bubble base radius d_w almost keeps constant. This means an increase in the curvature radius R and a decrease in gas phase contact angle of bubbles with the reduction in bubble height. In this case, the buoyancy force $\mathbf{F}_b$ and the contact pressure force $\mathbf{F}_{cp}$ increase based on equation 1. The drag force $\mathbf{F}_{qs}$ and the shear lift force $\mathbf{F}_{sl}$ on a bubble increase due to the increase in the term $R^2(u-v)|u-v|$ with the increase of R and u (a decrease in gas phase contact angle of bubbles contributes to drag reduction of fluid near the channel wall, leading to an increase in the fluid velocity u). As the hydrophobicity of channel wall increases, the pinning force $\mathbf{F}_p$ increases; while during the bubble sliding without detaching, $\mathbf{F}_p$ shows a decrease due to the reduction in bubble volume (Fig. S1b).

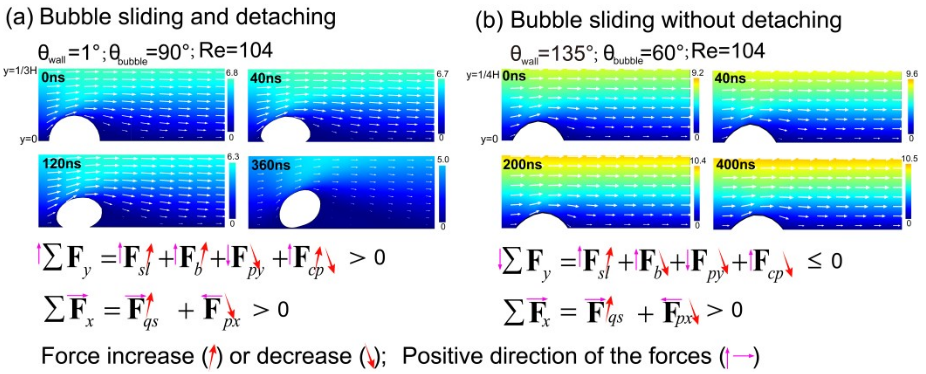

Figure S1 Analysis of the estimated force trends for surface bubble sliding and detaching (a) bubble sliding and detaching; (b) bubble sliding without detaching